



# Towards sustainability in the aerospace industry: Environmental impact of different drilling strategies for CFRP/Aluminium stacks

Martina Panico <sup>a</sup>, Ersilia Cozzolino <sup>a,\*</sup>, Antonello Astarita <sup>a</sup>, Eva Begemann <sup>b</sup>,  
Andreas Gebhardt <sup>b</sup>, Luca Boccarusso <sup>a</sup>

<sup>a</sup> Dept. of Chemical, Materials and Production Engineering, University of Naples "Federico II", P.le Tecchio 80, Naples 80125, Italy

<sup>b</sup> Fraunhofer Institute for Manufacturing Engineering and Automation IPA, Nobelstr. 12, Stuttgart 70569, Germany

## ARTICLE INFO

### Keywords:

Sustainability  
Sustainable manufacturing  
Drilling  
life cycle assessment  
Aerospace

## ABSTRACT

In the last decade improving the sustainability of manufacturing processes has become a primary objective to tackle the goals for sustainable development as defined by UN. In this context, the Life Cycle Assessment (LCA) is finding increasing use as a method to measure the environmental impacts of processes and as a tool to support decisions when a choice between different processing routes is required. The present study lies in this context: a detailed LCA analysis has been carried out to compare the environmental footprint of different drilling strategies, the quality of the drilled holes has also been considered to provide reliable guidelines to people interested in drilling operations. In particular, this study investigates the environmental impacts of different drilling strategies applied to CFRP/AA7075-T6 stacks, which are commonly used in structural aerospace assemblies. A cradle-to-gate LCA was performed to compare two main approaches: separate drilling of CFRP laminates and aluminium alloy sheets before their assembly, and one-shot drilling of pre-assembled stacks. A strength of this study, conversely to the others available in the literature, is that the analysis relies on experimental data for energy consumption, drilling forces and hole quality, enabling a high-fidelity environmental assessment. The results show that the drilling strategies significantly affect both the environmental indicators, process performance and hole quality, highlighting a trade-off between energy efficiency and hole characteristics. Findings offer new insight to guide sustainable decision-making in aerospace manufacturing.

## 1. Introduction

In the current industrial and academic landscape, sustainability has evolved from a conceptual ambition to a tangible operational imperative. The pressing need to reduce environmental impact both in terms of process efficiency and product design, has made methodologies like Life Cycle Assessment (LCA) essential tools for guiding informed and responsible decision-making. LCA, in fact, offers a structured framework for quantifying the environmental burdens associated with products and

processes across their life cycles, and its integration within manufacturing is rapidly gaining traction [1].

Among the numerous processes scrutinized through a sustainability lens, machining operations stand out for their widespread application and resource-intensive nature. Among these, milling [2–4] and turning [5–7] belong to the most studied processes, due to the significant amount of material removal, the extensive use of lubricants, the machining time involved, and the critical influence on tool life. Studies such as those by Herrero et al. [8] for milling and Fernando et al. [9] for

*Abbreviations:* ADPe, Abiotic Depletion Potential elements, [kg Sb eq.]; ADPf, Abiotic Depletion Potential fossil fuels, [kg Sb eq.]; AP, Acidification Potential, [kg CO<sub>2</sub> eq.]; EP, Eutrophication Potential, [kg P eq.]; GWP, Global Warming Potential, [kg CO<sub>2</sub> eq.]; ODP, Ozone Depletion Potential, [kg R11 eq.]; POCP, Photochemical Ozone Creation Potential, [kg C<sub>2</sub>H<sub>4</sub> eq.]; FAETP, Freshwater Aquatic Ecotoxicity Potential, [kg DCB eq.]; HTP, Human Toxicity Potential, [kg DCB eq.]; TETP, Terrestrial Ecotoxicity Potential, [kg DCB eq.]; CC, Climate change, [kg CO<sub>2</sub> eq.]; FPMF, Fine Particulate Matter Formation, [kg PM<sub>2.5</sub> eq.]; FD, Fossil depletion, [kg oil eq.]; FWC, Freshwater Consumption, [m<sup>3</sup>]; FWET, Freshwater Ecotoxicity, [kg 1,4-DB eq.]; FWEP, Freshwater Eutrophication, [kg P eq.]; HT<sub>c</sub>, Human toxicity, cancer, [kg 1,4 DB eq.]; HT<sub>nc</sub>, Human toxicity, non cancer, [kg 1,4 B eq.]; LU, Land use, [Annual crop eq. Yr]; MT, Marine toxicity, [kg 1,4 DB eq.]; ME, Marine Eutrophication, [kg N eq.]; MD, Metal depletion [kg Cu eq.], [kg Cu eq.]; POF<sub>e</sub>, Photochemical Ozone Formation, Ecosystem, [kg Nox eq.]; POF<sub>h</sub>, Photochemical Ozone Formation, human Health, [kg Nox eq.]; SOD, Stratospheric Ozone Depletion, [k CFC-11 eq.]; TA, Terrestrial Acidification, [kg SO<sub>2</sub> eq.].

\* Corresponding author.

E-mail address: [ersilia.cozzolino@unina.it](mailto:ersilia.cozzolino@unina.it) (E. Cozzolino).

<https://doi.org/10.1016/j.cirpj.2025.12.001>

Received 21 May 2025; Received in revised form 28 November 2025; Accepted 1 December 2025

Available online 5 December 2025

1755-5817/© 2025 The Author(s). This is an open access article under the CC BY license (<http://creativecommons.org/licenses/by/4.0/>).

turning have shown how lubrication and process optimization can considerably reduce energy consumption and environmental impacts while improving the overall sustainability of machining operations.

Drilling processes, at first glance, might seem less critical due to their generally shorter execution times. However, their impact becomes highly relevant depending on the industrial sector considered. Although drilling may appear as a niche operation, it becomes environmentally impactful when applied to large-scale assemblies, such as in the aerospace sector. For instance, the production of a single aircraft fuselage can involve the drilling of over 60,000 holes for medium-sized commercial aircraft, each influencing structural integrity and assembly logistics [10,11].

Within this context, drilling plays a pivotal role in the assembly of structural components through-bolted and riveted joints [12,13]. Particularly, hybrid structures combining CFRP and aluminium alloys [14], or CFRP and titanium alloys [15], have become increasingly fundamental. Depending on the adopted production strategy, drilling operations may be performed either individually on each component before assembly or in a stacked configuration where multiple layers are drilled simultaneously. The latter approach further complicates the process due to the heterogeneous nature of the cutting conditions imposed by dissimilar materials [16].

Traditionally, research in this field has focused on optimizing drilling to meet stringent mechanical performance and quality criteria. As reviewed by Xu et al. [17], significant efforts have been devoted to studying the influence of cutting parameters, tool geometry, and lubrication strategies on outcomes such as thrust force, torque, surface quality, burr formation, delamination, tool wear, and dimensional accuracy.

However, despite the increasing attention to sustainable manufacturing, the environmental implications of drilling have been only marginally explored. The application of LCA methodologies has been limited, mainly focusing on the effects of lubrication and cooling strategies on environmental indicators. For example, Campitelli et al. [18] compared the environmental performance of Flood Lubrication (FL) and Minimum Quantity Lubrication (MQL) during drilling and milling operations of aluminium, steel, and cast iron, highlighting a significant reduction in resource consumption and energy demand when adopting MQL. Similarly, Khanna et al. [19] and Shah et al. [20] investigated drilling operations under different cooling conditions, showing that cryogenic and dry drilling can reduce energy consumption and fluid waste management, though they also identified the environmental costs associated with cryogenic fluid production.

Even less attention has been devoted to composite materials. Recently, Khanna et al. [21], for example, conducted one of the few LCA studies on hybrid titanium composite laminates drilled in dry and CO<sub>2</sub> cryogenic environments. Other rare examples include studies such as those of Zhu et al. [22,23] where the authors analysed the energy consumption and environmental impact associated with drilling carbon fibre reinforced polymers (CFRPs), highlighting how drilling parameters and stack configurations significantly influence both machining efficiency and ecological footprint. Additionally, Kang et al. [24] examined the environmental impact of drilling CFRP/aluminium stacks, emphasizing the importance of process optimization in reducing energy consumption and associated emissions.

Nevertheless, like metals, the focus of these studies has largely been on analysing the effects of cutting parameters and lubrication on process sustainability.

A significant gap remains in the literature regarding the environmental assessment of drilling strategies for stacked structures commonly used in aerospace applications. In this context, it becomes crucial to also study how drilling strategies, as broader methodologies encompassing how components are drilled and assembled, affect sustainability. To date, such strategies have received little to no attention in LCA frameworks. This represents a critical knowledge gap, especially in aerospace manufacturing, where the choice between single material and stacked

drilling configurations directly impacts not only the sustainability of the drilling process, but also the assembly strategy, the number of pre-assembly operations required and the overall production complexity.

This work aims to bridge this gap by investigating the environmental impact of different drilling strategies applied to aerospace structural assemblies, with a particular focus on hybrid stacks composed of CFRP and AA7075-T6 aluminium alloy. In such hybrid stacks, the interaction between dissimilar materials during drilling generates highly heterogeneous cutting conditions, which in turn affect both, hole quality and energy consumption [16,14].

To address this multifaceted problem, a cradle-to-gate LCA was conducted comparing two manufacturing scenarios: (i) separate drilling of CFRP and AA7075-T6 components followed by assembly; and (ii) one-shot drilling of pre-assembled CFRP/AA stacks. Unlike previous studies relying on database estimates, this research leverages experimental data for both energy monitoring and quality assessment, ensuring high-fidelity environmental modelling. Moreover, the analysis does not merely compare process parameters, it explicitly evaluates the impact of different drilling strategies on both energy performance and final product quality. The results achieved will be combined and discussed aiming to provide insights on the sustainability of these processes and give useful guidelines for carrying out these operations on an industrial scale.

## 2. Materials and methods

The present study is based on the experimental results previously obtained and discussed by Panico et al. [25] on the drilling of CFRP/AA7075-T6 stacks. Both the condition in which the materials are drilled individually and the one-shot drilling strategy were investigated. In that work, an innovative drilling strategy was implemented, based on the online monitoring of spindle active power to dynamically adapt the cutting parameters across the material interface. This parameter-switching methodology, triggered by characteristic variations in the active power signal, allowed the tool to seamlessly transition from the CFRP to the AA7075-T6 layer, ensuring optimal process conditions for each material. The results highlighted the ability of this adaptive strategy to mitigate typical interface defects, such as delamination in CFRP and burr formation in AA7075-T6. Specifically, the results concerning active power consumption and hole quality indicators, gathered during that experimental campaign, were adopted as primary data of the Life Cycle Impact Assessment (LCIA) conducted in this work.

### 2.1. Materials and machine tool specifications

The subject of this study is the drilling of a hybrid stack composed of a quasi-isotropic CFRP laminate (3.6 mm in thickness and a symmetric lay-up of [90/−45/0/45/90/−45/0/45]<sub>s</sub>) and an AA7075-T6 aluminium alloy sheet of 4.0 mm in thickness, resulting in a total stack thickness of 7.6 mm when assembled. The specimens have in-plane dimensions of 100 mm × 200 mm.

In the stack, the CFRP laminate was always placed on top of the aluminium plate in accordance with industrial requirements and scientific literature [26].

All drilling tests were carried out using a five-axis CNC machining centre (Reichenbacher ECO-LT 2012), under dry cutting conditions. The drilling tool used was a solid carbide twist drill with a diameter of 4.84 mm, a 120° point angle and a CVD diamond-coating. The specimens were securely clamped between two steel plates using six dowel pins to ensure accurate positioning and repeatable boundary conditions during drilling. The slots in the clamping plates were dimensioned with a width slightly larger than the nominal hole diameter, in order to limit out-of-plane deflection and avoid stack separation during drilling, while preserving the integrity of the stack interface.

The experimental campaign included an integrated system for real-time monitoring of spindle active power. The electrical power

consumption of the spindle motor was continuously measured using a Hall-effect-based sensor system (Nordmann WLM-3s). The system configuration, illustrated in Fig. 1, consisted of three current sensors mounted on the u, v, and w phases of the spindle motor, enabling the acquisition of instantaneous current and voltage signals. These measurements were processed by a dedicated control unit (SEM-Modul-e) to compute the active power absorbed by the spindle during the drilling process. The SEM-Modul-e unit was connected to the numerical control unit (NCU) of the CNC machine via an analogue input, enabling the automated adaption of an ongoing drilling process, such as automatic parameter switching, by analysing the dynamic behaviour of the active power curve. Specifically, the integration scheme of the power monitoring system and the experimental setup is schematically depicted in Fig. 1. For the force system analysis, the thrust force ( $F_z$ ) and torque ( $M_z$ ) were acquired using the KISTLER 9272 dynamometer (see Fig. 1). The dynamometer was then connected to the charge amplification and data acquisition system for multi-component force-torque measurement, KISTLER 5167A41KH2.

## 2.2. Drilling process parameters and strategies

When each material was individually drilled prior to assembly (this strategy will hereafter be referred to as the single-material drilling strategy), a full-factorial experimental design was adopted, as described in the experimental campaign described by Panico et al. [25]. This included three levels of cutting speed ( $v_c$ ) and three levels of feed rate ( $f$ ), resulting in nine parameter combinations per material. Three holes were drilled for each combination and to ensure that the drilling results in terms of measured forces, quality and energy consumption were not affected by wear effects, for each combination test a new tool was used.

When the one-shot strategy was adopted, two different approaches

were implemented. The first involved the application of a single set of cutting parameters ( $v_c$  and  $f$ ) throughout the entire stack thickness, regardless of the material being drilled. The second approach consisted in modifying the cutting parameters in real time at the interface between the two materials. In agreement with the approach proposed in [25], the transition from the CFRP to the aluminium cutting parameters was triggered based on the evolution of the active power signal and was applied when the cutting edge was fully engaged in the AA7075-T6 layer. Six holes were drilled for each drilling condition, for each one a new tool was used.

For the LCA, a subset of nine representative drilling conditions was extracted from the complete experimental campaign. These combinations were selected to represent distinct operational scenarios and selection criteria relevant to both manufacturing practice and environmental impact analysis.

For AA7075-T6 and CFRP drilled in single-material strategy, three process conditions were selected per material:

- A condition optimised for best hole quality (BHQ), based on minimal burr formation (AA7075-T6) or minimal delamination (CFRP);
- A condition associated with minimum active power consumption (MnAP);
- A condition representative of the maximum active power level (MxAP), defined as the parameter combination that produced the highest peak value of active power during the drilling operation.

For the CFRP/AA7075-T6 stacks, the selected conditions included:

- Two compromise strategies. One of these combinations was defined to favour the AA7075-T6 drilling conditions (labelled as CP-AA in Table 1), while the other was selected to favour the CFRP (labelled as

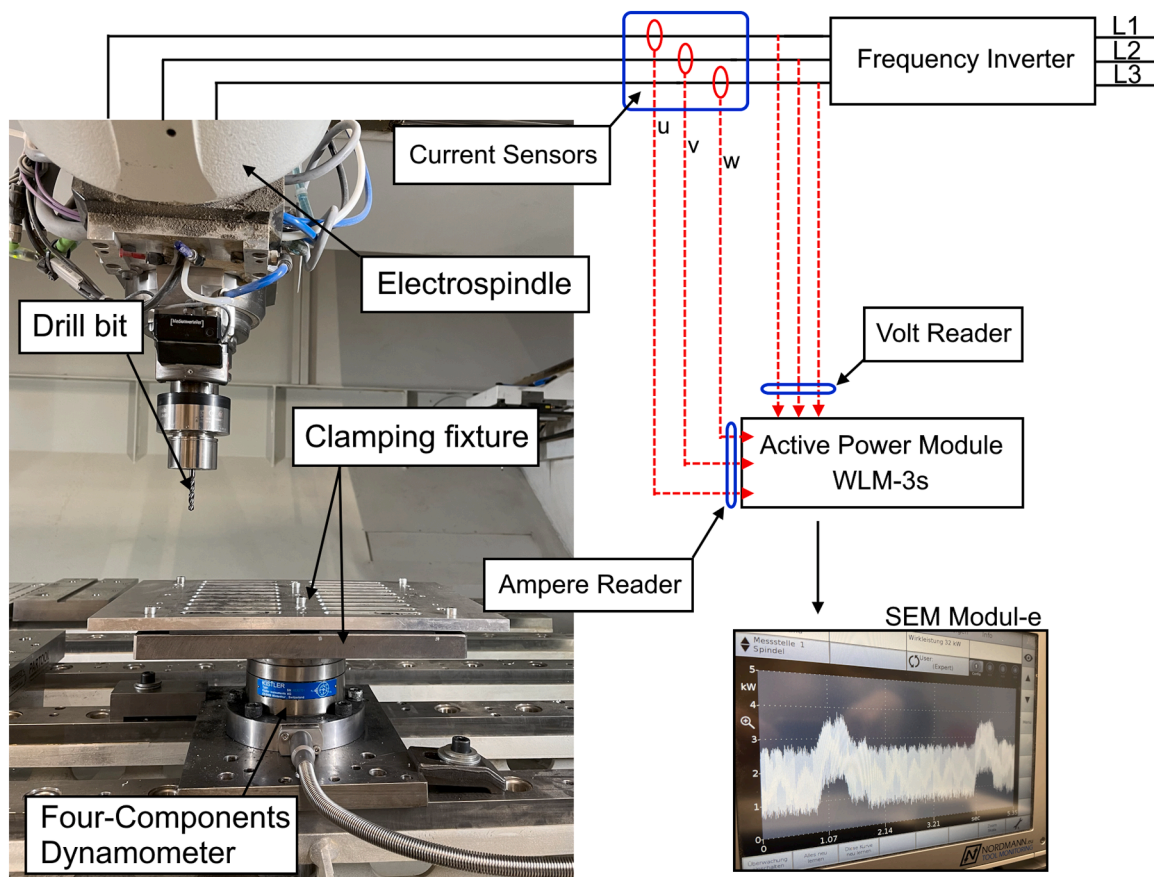


Fig. 1. Experimental setup and integration scheme of the power monitoring system used during drilling tests.

**Table 1**

Summary of the drilling process parameters and corresponding selection criteria considered for the LCA.

Drilling Strategy	Materials	$v_c$ [m/min]	$f$ [mm/rev]	$n$ [rpm]	$v_a$ [mm/min]	MRR [ $\text{mm}^3/\text{min}$ ]	Selection Criterion
Single material	AA7075-T6	60	0.075	3946	295.95	5445.44	BHQ
Single material	AA7075-T6	60	0.050	3946	197.30	363.0	MnAP
Single material	AA7075-T6	140	0.125	9207	1150.91	21,175.0	MxAP
Single material	CFRP	85	0.010	5590	55.90	1028.50	BHQ
Single material	CFRP	50	0.010	3288	32.88	605.0	MnAP
Single material	CFRP	120	0.070	7892	552.44	10164.0	MxAP
One-Shot	CFRP/AA7075-T6	60	0.075	3946	295.95	5445.0	CP-AA
One-Shot	CFRP/AA7075-T6	80	0.050	5261	263.06	91.68	CP-CFRP
One-Shot	CFRP/AA7075-T6	85/60	0.010/0.075	5590/3946	55.90/295.95	1028.45/5445.44	APS

CP-CFRP in Table 1). Specifically, these compromise combinations were derived from the results analysed in [25]: CP-AA adopts cutting parameters (lower cutting speed and higher feed rate) that had proven effective for AA7075-T6 in minimising burr formation, while CP-CFRP is based on parameters (higher cutting speed and lower feed rate) that were found beneficial for CFRP in reducing delamination and thrust force.

- The adaptive parameter switching strategy, corresponding to the switching identified in [25] as the optimal switching condition in terms of hole quality and process stability (labelled as APS in Table 1).

The drilling conditions considered in this study are summarised in Table 1.

Among the reported parameters, the Material Removal Rate (MRR) was also calculated using the following expression:

$$MRR = \pi \left( \frac{d^2}{4} \right) f n \tag{1}$$

where  $d$  is the tool diameter,  $f$  is the feed per revolution, and  $n$  is the spindle speed.

### 2.3. Process monitoring: thrust force, power and energy consumption

Energy consumption associated with each drilling condition was derived from the active power signal acquisitions carried out on the spindle motor during the drilling process as described in Section 2.1.2.

The collected data were subsequently used to compute the total energy consumption ( $E_{TOT}$ ) for each drilling operation.  $E_{TOT}$  related to each drilling operation was computed as the sum of two distinct contributions, as follows:

$$E_{TOT} = E_{CNC} + E_{motor} = P_{CNC,ave} \cdot T_{drilling} + \int_0^{T_{drilling}} P_{active}(t) \cdot dt$$

$$\approx P_{CNC,ave} \cdot T_{drilling} + \sum_{i=1}^{T_{drilling}/\Delta t} P_{active,i} \cdot \Delta t \tag{2}$$

Where:

- $E_{CNC}$ , which is the energy demand of the CNC auxiliary systems (e.g., positioning movements, electronics), was assumed constant and estimated as the product of the average power consumption ( $P_{CNC,ave}$ ) and the nominal drilling time ( $T_{drilling}$ ). The power consumption of the CNC machine was considered constant throughout the entire drilling operation and equal to 23 kW ( $P_{CNC,ave}$ ), in accordance with the CNC machine technical datasheet. Nominal power of the CNC auxiliary systems indicated in the technical datasheet was used to calculate the  $E_{CNC}$ . although this assumption may slightly overestimate the absolute value of  $E_{CNC}$ , it does not affect the comparative nature of the study since the same hypothesis is consistently applied across all scenarios.

- $E_{motor}$ , which is the energy absorbed by the spindle motor during the entire drilling operation. It was calculated by integrating the measured active power signal over the drilling time, as shown in Eq. 2, with the variables defined below.
- $\Delta t$  is the sampling period, equal to 0.002 s and  $P_{active,i}$  is the active power taken every 0.002 s, from the beginning to the end of the drilling process ( $T_{drilling}$ ) whose signal was acquired from the spindle motor. It includes two distinct contributions:

- $P_{air}$ , identified as air cut power, corresponding to the power required to maintain the spindle rotation without any tool-workpiece engagement, measured when the tool moves in air while the entire CNC system is active.
- $P_{cut}$ , corresponding to the net power demand for material removal, calculated as the difference between the actual active power and the air cut power, in agreement with the literature [27]:

$$P_{cut} = P_{active} - P_{air} \tag{3}$$

Fig. 2 shows a representative active power curve for each material: single-material drilling strategy of AA7075-T6 (Fig. 2a), CFRP (Fig. 2b), and one shot drilling strategy of CFRP/AA7075-T6 stacks (Fig. 2c).

For each curve, the total energy associated with the spindle motor ( $E_{motor}$ ) was graphically decomposed into two terms:

- Air cutting energy contribution ( $E_{air}$ ), corresponding to the energy required to maintain spindle rotation without material engagement. This contribution was calculated by multiplying the air cut power ( $P_{air}$ ) by the drilling time.
- Cutting energy contribution ( $E_{cut}$ ), corresponding to the additional energy required to remove the material. This contribution is associated with the cut power ( $P_{cut}$ ), which varies depending on the interaction between the tool and the material.

Furthermore, the Specific Cutting Energy (SCE) was calculated for each drilling condition as an additional parameter to assess the energy efficiency of material removal. SCE represents the amount of energy required to remove a unit volume of material and is defined as the ratio between the average cutting power  $\bar{P}_{cut}$  and the material removal rate (MRR):

$$SCE = \frac{\bar{P}_{cut}}{MRR} \tag{4}$$

$\bar{P}_{cut}$  was computed by isolating the stationary segment of the cutting phase within the active power signal and performing a mean value integrating over that interval. The MRR is reported for each drilling strategy in Table 1.

In addition, the maximum thrust force was extracted from the force signal acquired during each test. For the single-material drilling strategy, a single peak thrust force value was identified per material. In the case of hybrid stacks, the maximum thrust force was separately identified for each material interface, reflecting the distinct cutting behaviour

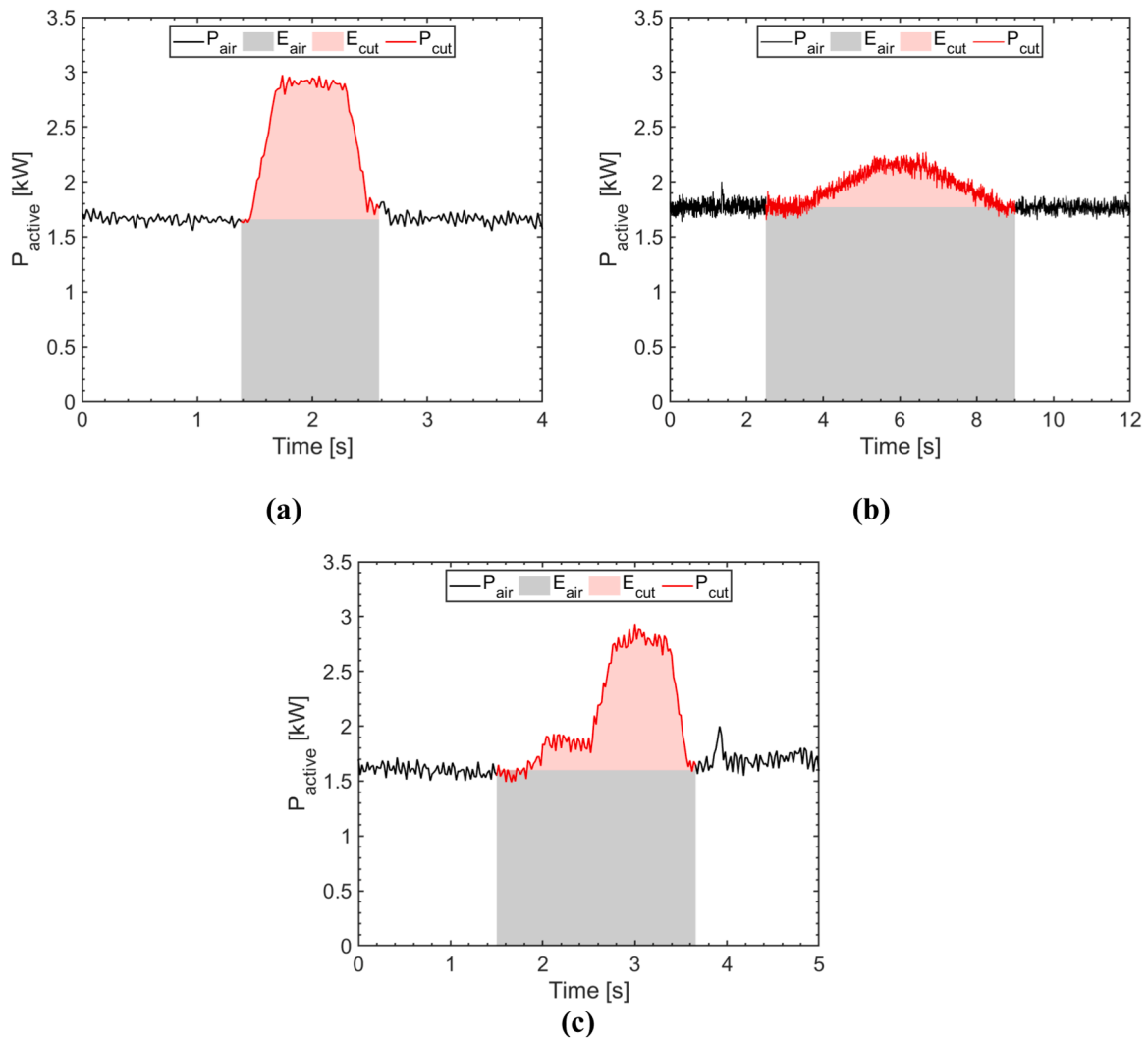


**Fig. 2.** Representative active power curves acquired from the spindle motor during the drilling operations for the three selected strategies: (a) single-material drilling strategy of AA7075-T6, (b) CFRP, and (c) one-shot drilling strategy of CFRP/AA7075-T6 stack.

at different depths. To support this analysis, by way of example Fig. 3a shows the thrust force evolution during the drilling of AA7075-T6 and CFRP in single-material strategy under the MnAP conditions. Fig. 3b, instead, compares the thrust force signals acquired during drilling under CP-AA, CP-CFRP and APS conditions in the one-shot drilling strategy. Each thrust force curve in Fig. 3b has been segmented to distinguish the time intervals corresponding to the drilling of the CFRP and the AA7075-T6, respectively. In the case of the single-material drilling strategy (Fig. 3a), it can be observed that the peak thrust force recorded during AA7075-T6 drilling is approximately 3.5 times higher than that observed in the CFRP. Such a result is consistent with trends commonly reported in the literature for drilling dissimilar materials [16,28,29]. When considering the one-shot drilling strategy, the material-driven nature of the thrust force remains evident, with peak values systematically higher in the AA7075-T6 section across all strategies. However, small variations in peak thrust force values can be noticed even when the same material is drilled, as in the case of CFRP in Fig. 3a and Fig. 3b. These differences mainly attributable to the process parameters and drilling strategies (single-material drilling or one-shot drilling). For instance, in the APS strategy, CFRP is drilled using the same feed rate (0.01 mm/rev) as in the MnAP condition, but with a higher cutting speed (85 m/min vs 50 m/min). According to Panico et al. [25], increasing cutting speed slightly reduces the thrust force. Nonetheless, in APS, the CFRP layer lies above a stiff AA7075-T6 backing layer, which

effectively increases the global stiffness of the laminate during drilling, resulting in a higher thrust peak compared to the monolithic configuration. This interaction reduces the beneficial effect of increasing cutting speed, explaining the higher thrust force despite the use of more favourable cutting parameters. Furthermore, even for the CP-AA and CP-CFRP combinations, higher thrust force peaks are recorded during CFRP drilling (around 46 N and 41 N, respectively) compared to the MnAP combination (around 30 N). This increase, in addition to the drilling strategy adopted, is mainly attributable to the higher feed rates used (0.075 and 0.050 mm/rev versus 0.01 mm/rev), which cause an increase in thrust force, as widely documented in the literature [30–32]. Additionally, the significant variation observed in the peak thrust force of AA7075-T6 between CP-AA and CP-CFRP conditions (around 125 N and 92 N, respectively) can be attributed to the different process parameters adopted. Specifically, CP-AA was executed with a lower cutting speed ( $v_c = 60$  m/min) and higher feed rate ( $f = 0.075$  mm/rev), while CP-CFRP used a higher cutting speed ( $v_c = 80$  m/min) and a lower feed rate ( $f = 0.050$  mm/rev). As also confirmed in [25], thrust force tends to increase with increasing feed rate, while a rise in cutting speed typically reduces the force due to thermal softening of the material. The higher thrust force in CP-AA is thus the combined effect of a more aggressive feed rate and a reduced cutting speed. Finally, the APS condition shows a shorter duration of the peak thrust force in the AA7075-T6 layer compared to CP-AA and CP-CFRP. This is attributable to the fact that, in

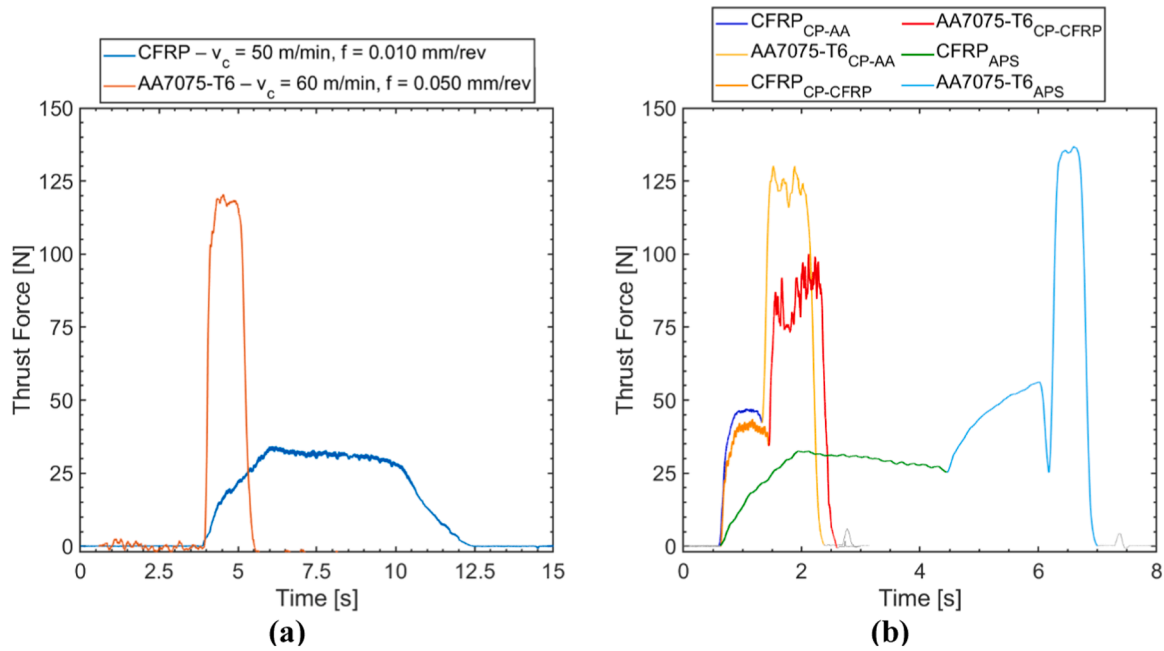


Fig. 3. Thrust force evolution during (a) drilling of CFRP and AA7075-T6 under MnAP conditions in single-material drilling strategy; (b) one shot drilling of the stack drilled in CP-AA, CP-CFRP, and APS conditions. The corresponding process parameters are reported in Table 1.

APS, the upper portion of the aluminium thickness is drilled using parameters optimised for CFRP, including a much lower feed rate ( $f = 0.01$  mm/rev). Moreover, it is worth noting that in the APS condition, due to the use of CFRP-optimised parameters during the first portion of the stack, the overall drilling time is significantly longer compared to CP-AA and CP-CFRP, where more aggressive, constant parameters are applied throughout. This is reflected in the extended duration of the thrust force signal in the APS curve.

The main values of drilling time, energy consumption, SCE and thrust force for all selected conditions are summarised in Table 2.

#### 2.4. Life Cycle Assessment (LCA)

A cradle-to-gate LCA has been carried out to compare the environmental impact of drilling AA7075-T6 and CFRP in single-material drilling strategy with the one-shot drilling strategy of the stack described in the previous sections (Table 1). LCA for Experts Solutions (Sphera – ex GaBi) software has been used to perform the LCA analyses according to the international standards ISO 14040 [33]- 14044 [34].

These international standards do not specify a single method for the Life Cycle Impact Assessment (LCIA) analysis. Currently, different methods exist in this regard and the choice between them is not always obvious. In this work, either CML 2016 and ReCiPe 2016 v1–1- Midpoint (H) methods were selected to perform the LCIA to compare the results obtained and eventually identify discrepancies and similarities between them [35].

Table 2  
Drilling time and energy consumption data associated with the selected drilling conditions.

Selection Criterion	Materials	$T_{drilling}$ [s]	$P_{CNC,ave}$ [kW]	$E_{CNC}$ [kJ]	$E_{motor}$ [kJ]	$E_{TOT}$ [kJ]	Thrust Force [N]	SCE [J/mm <sup>3</sup> ]
BHQ	AA7075-T6	1.20	23.00	27.60	3.04	30.64	148.71	14.66
MnAP	AA7075-T6	1.76	23.00	40.48	4.15	44.63	116.15	15.80
MxAP	AA7075-T6	0.46	23.00	10.58	2.00	12.58	234.82	11.57
BHQ	CFRP	6.51	23.00	149.64	12.75	162.39	31.62	22.95
MnAP	CFRP	5.59	23.00	128.52	8.79	137.31	31.71	30.74
MxAP	CFRP	0.70	23.00	16.10	1.85	17.95	48.97	4.61
CP-AA	AA7075-T6/CFRP	2.16	23.00	49.68	4.63	54.31	46.44/124.85	3.07/13.37
CP-CFRP	AA7075-T6/CFRP	2.50	23.00	57.50	6.23	63.73	41.29/91.68	16.15/71.12
APS	AA7075-T6/CFRP	6.00	23.00	138.00	13.31	151.31	38.01/138.86	22.36/13.31

In the following subsections, the goal and scope of the carried out LCAs, as well as the data inventories used, were defined.

##### 2.4.1. Goal and scope definition

The purpose of the LCA carried out in this work is to compare two main operational scenarios of the aerospace industry:

- I) Assembly of AA7075-T6 sheet and quasi-isotropic CFRP laminate drilled using the single-material drilling strategy.
- II) Assembly of CFRP/AA7075-T6 stacks drilled in one-shot strategy.

For each scenario, three different drilling process conditions have been investigated. In particular, for scenario I, the following sub-scenarios were investigated according to Table 1:

- I.A) Best hole quality AA7075-T6 + best hole quality CFRP ( $v_c = 60$  m/min and  $f = 0.075$  mm/rev for AA7075-T6 and  $v_c = 85$  m/min and  $f = 0.010$  mm/rev for CFRP);
- I.B) Minimum active power AA7075-T6 + minimum active power CFRP ( $v_c = 60$  m/min and  $f = 0.050$  mm/rev for AA7075-T6 and  $v_c = 50$  m/min and  $f = 0.010$  mm/rev for CFRP);
- I.C) Maximum active power AA7075-T6 + maximum active power CFRP ( $v_c = 140$  m/min and  $f = 0.125$  mm/rev for AA7075-T6 and  $v_c = 120$  m/min and  $f = 0.070$  mm/rev for CFRP).

Instead, for scenario II, the following subscenarios were investigated:

- II. A) Compromise parameters – CP-AA ( $v_c = 60$  m/min and  $f = 0.075$  mm/rev);
- II. B) Compromise parameters – CP-CFRP ( $v_c = 80$  m/min and  $f = 0.050$  mm/rev);
- III. C) Adaptive parameter switching strategy ( $v_c = 85$  m/min and  $f = 0.010$  mm/rev for CFRP and  $v_c = 60$  m/min and  $f = 0.075$  mm/rev for AA7075-T6).

Fig. 4 displays the schematization of the scenarios investigated. A cradle-to-gate analysis has been carried out, going from the raw material production to the final assembly. The main differences between the two scenarios lie in the workflow adopted for the drilling and assembly phase. In scenario I, drilling operations are carried out separately on the individual components, which are then subjected to a dedicated cleaning phase and subsequently assembled. This approach requires two distinct drilling steps, one for each material, prior to final joining. In contrast, Scenario II involves a drilling strategy performed on the stacked components. To enable accurate positioning and prevent relative displacement during the drilling operation, a pre-assembly phase is required. In aerospace sector, this typically consists of the creation of pilot holes (with a smaller diameter than the final one) to accommodate temporary fasteners, which ensure proper alignment and clamping of the parts prior to final drilling and joining. This difference in workflow

represents a key motivation of the present study: the comparison between Scenario I and Scenario II is intended to assess whether, and to what extent, these variations influence the overall environmental impact of the assembly process.

To account for the additional energy required in Scenario II due to the pre-assembly phase, the total energy consumption ( $E_{TOT}$ ) for the realisation of each pilot hole ( $\varnothing 3.30$  mm) accommodating the temporary fasteners was estimated. Following the same approach adopted for standard drilling operations,  $E_{TOT}$  was considered as the sum of  $E_{CNC}$  and the spindle motor energy  $E_{motor}$ . While  $E_{CNC}$  was computed as the product of the average CNC power and the nominal drilling time,  $E_{motor}$  was estimated by scaling the measured energy from an actual drilling condition. Specifically, the energy reference was taken from MxAP conditions. Given that no physical pilot holes were drilled in the experimental campaign, the actual energy was estimated proportionally from the measured  $E_{motor}$  value of MxAP condition (performed on  $\varnothing 4.84$  mm) using the following time-based relation:

$$\frac{T_{drilling,real}}{E_{motor,real}} = \frac{T_{drilling,pilot}}{E_{motor,pilot}} \tag{5}$$

The estimation was performed separately for CFRP and AA7075-T6, considering their respective drilling times.

The definition of a Functional Unit (FU) is necessary for modelling a

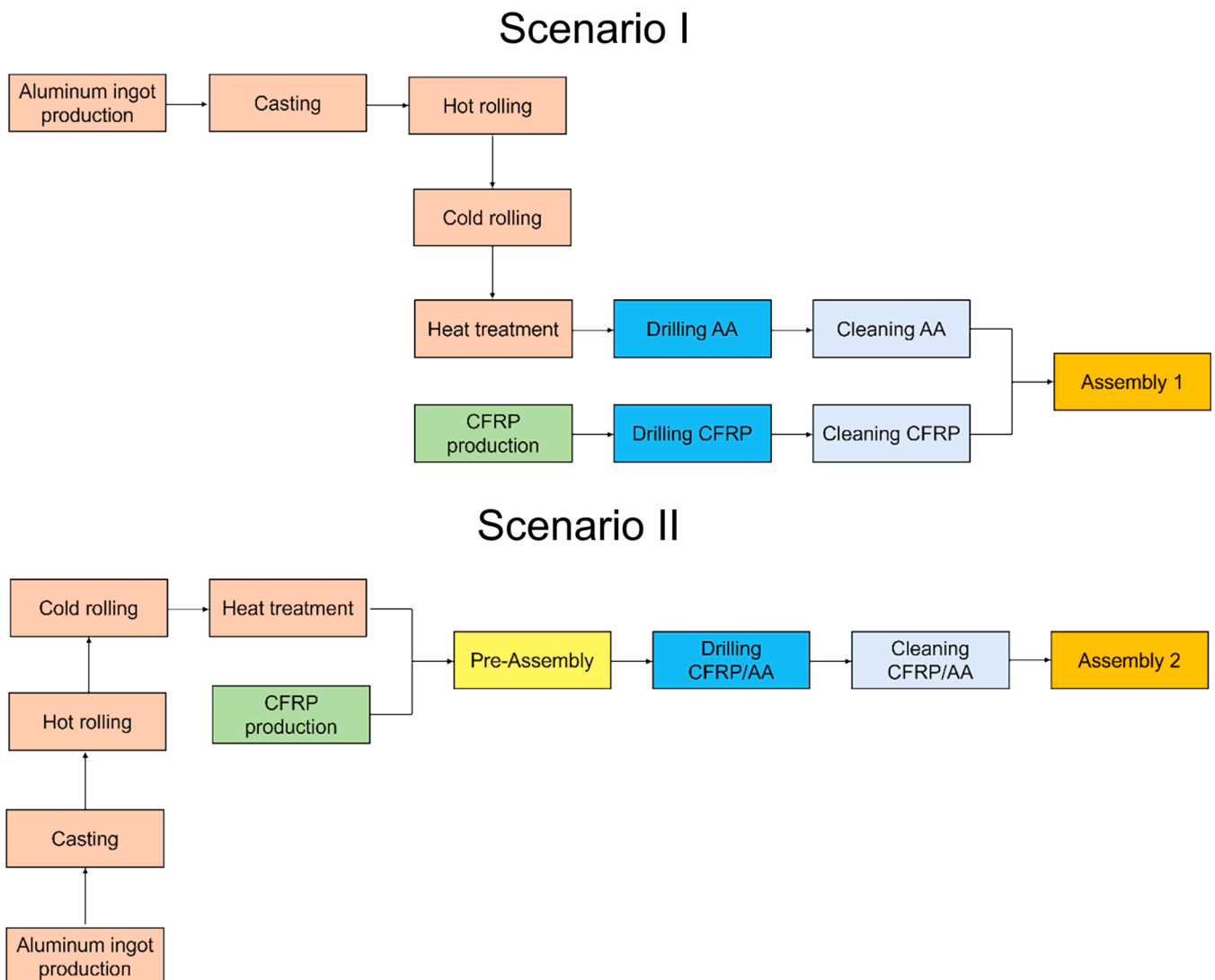


Fig. 4. Schematization of the scenarios investigated in this work.

product system in the LCA. A FU is typically a quantified description of the function of a product that serves as the reference basis for all calculations and comparison of the environmental impact assessment.

The FU chosen for the LCA scenarios carried out in this work is the standardized control volume of a drilled panel, having a hole diameter  $D$  of 4.84 mm, as schematized in Fig. 5. According to the standards, it is required to maintain a fastener spacing approximately four times the fastener diameter ( $d$ ) or more.

On these premises, the FU for all the scenarios and subscenarios of this work is the control volume A, indicated in red in Fig. 5. It has a volume of  $60 \times 20 \times t$  mm<sup>3</sup>, where  $D = 4.84$  mm,  $d = 19.36$  mm, and  $t$  is the final thickness of the panel as a consequence of the CFRP/AA7075-T6 assembly. In Scenario II, considering the extent of the control volume, two temporary fasteners were assumed to be required to ensure the relative positioning of the stacked layers during the pre-assembly phase. This FU was selected because drilling is not an isolated operation in aerospace manufacturing, but part of a wider assembly workflow in which hole spacing, pre-assembly and joining must all be accounted for

These analyses aim to identify potential hot spots and environmental benefits in the drilling of CFRP/AA7075-T6 stacks in one-shot strategy rather than the individual drilling of AA7075-T6 and CFRP laminate before their assembly.

2.4.2. Life cycle inventory (LCI)

All the input and output fluxes of all the processes modelled within the system boundaries were quantified and collected to build the Life Cycle Inventory (LCI) of all the scenarios investigated in this work. Primary data were derived from direction measurements, whereas secondary data were collected from the Ecoinvent 3.1 database within the LCA software adopted, calculations derived from the technical datasheet of the resources used, or literature. Some assumptions have been made in this work. In particular, transportation was not included in the analyses, considering that all the processes included in all the scenarios were performed in the same location, except for the production processes of the two materials involved.

Also, machine production was considered out of the system boundaries, as, due to their long service life, they would have a negligible impact on the drilling of a single hole. To decide whether the processes have to be included in the LCA, a cut-off level of 1 % has been applied [36].

Data to model CFRP production and Aluminum ingot production were derived from the available literature [37,38]. In particular, for the realization of the aluminum sheets, all the following stages have been included in the modelling: aluminum production, casting, hot rolling, cold rolling, heat treatment.

Resources' data used to model the drilling, cleaning and assembly stages derived from experimental measurements (EM), calculations derived from technical datasheet (TD), software database (SD), as indicated in the following LCI Tables, which refer to the FU selected in this work mentioned above and illustrated in Fig. 5. That means that all

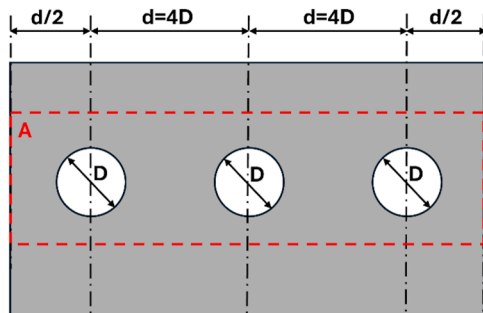


Fig. 5. Schematization of the FU – the standardized control volume A – chosen for the LCA.

the resources quantified in the LCI Tables are those needed to obtain the final drilled panel.

In particular, Table 3 and Table 4 contain the inventory data used for modelling the drilling and cleaning, respectively, of AA7075-T6 in the I, A, I.B and I.C subscenarios. Similarly, Table 5 and Table 6 contain data used for modelling the CFRP drilling and cleaning, respectively, of the same subscenarios. Table 7 contain data of the assembly 1, as indicated in Fig. 3, thus of the assembly of AA7075-T6 and CFRP after the drilling and the cleaning of each material for all the subscenarios of scenario I.

The flux indicated as “Aluminum rivet [pcs]” in Table 7 indicates the aluminum riveting which was performed in the final assembly of all the scenarios: to this purpose, Ecoinvent 3.1 database was used, including all the resources involved (material, compressed air, and energy for compressed air).

In the scenario II, the drilling process of the stack CFRP/AA7075-T6 was anticipated by a pre-assembly, whose data used for the LCA are contained in Table 8. Temporary fasteners were used during pre-assembly, drilling, and cleaning stages. The addition of the temporary fasteners before the drilling process led to the presence of pilot holes and, thus, to a reduction of the weight of the material to be drilled, which is the stack CFRP/AA7075-T6, differently to the scenario I. That explains the difference in the material’s weight to be drilled comparing I and II scenarios. The total energy consumption required for drilling the pilot holes was calculated according to Eq. 5 and reported in Table 8.

3. Results and discussion

3.1. Life Cycle Impact Assessment (LCIA)

Diagrams in Fig. 6 and Fig. 7 enable to visualize the most affected environmental impact categories according to CML method and ReCiPe 2016, for all the investigated scenarios. In particular, for the CML method, they are:

- ADP<sub>f</sub>, which is the Abiotic Resources Depletion (fossil), and measures the over-extraction of fossil fuels including all fossil resources.
- GWP, which is representative of the Global Warming Potential, and quantifies the kg of the carbon dioxide equivalent
- HTP, which is the Human Toxicity Potential and reflects the potential harm of a unit of chemical released into the environment, is based on both the inherent toxicity of a compound and its potential dose.

For ReCiPe 2016, the most affected environmental categories are:

- CC, which represents the Climate change. It is the equivalent of the GWP for the CML method.

Table 3  
LCI of drilling AA7075-T6.

Resources	Data	INPUT (I)/ OUTPUT (O)	I.A	I.B	I.C
Total energy consumption for drilling AA7075-T6 [kJ]	EM	I	3.06E+ 01	4.46E+ 01	1.26E+ 01
AA7075-T6 part [kg]	EM	I	1.24E-02	1.24E-02	1.24E-02
Drilled AA7075-T6 part [kg]	EM	O	1.22E-02	1.22E-02	1.22E-02
Energy for compressed air [kJ]	EM	I	4.14E+ 00	6.07E+ 00	1.59E+ 00
Compressed air [m <sup>3</sup> ]	TD	I	1.80E-01	2.64E-01	6.90E-02
AA7075-T6 scrap [kg]	EM	O	1.90E-04	1.90E-04	1.90E-04

**Table 4**  
LCI of cleaning AA7075-T6.

Resources	Data	INPUT (I)/ OUTPUT (O)	I.A	I.B	I.C
Drilled AA7075-T6 part [kg]	EM	I	1.22E-02	1.22E-02	1.22E-02
Cleaned AA7075-T6 part [kg]	EM	O	1.22E-02	1.22E-02	1.22E-02
Compressed air [m <sup>3</sup> ]	TD	I	1.33E-02	1.33E-02	1.33E-02
Energy for compressed air [kJ]	EM	I	3.06E-01	3.06E-01	3.06E-01

**Table 5**  
LCI of drilling CFRP.

Resources	Data	INPUT (I)/ OUTPUT (O)	I.A	I.B	I.C
Total energy consumption for drilling CFRP [kJ]	EM	I	1.62E+ 02	1.37E+ 02	1.79E+ 01
CFRP part [kg]	EM	I	7.32E-03	7.32E-03	7.32E-03
Drilled CFRP part [kg]	EM	O	7.21E-03	7.21E-03	7.21E-03
Energy for compressed air [kJ]	EM	I	2.24E+ 01	1.93E+ 01	2.42E+ 00
Compressed air [m <sup>3</sup> ]	TD	I	9.76E-01	8.38E-01	1.05E-01
CFRP scrap [kg]	EM	O	1.12E-04	1.12E-04	1.12E-04

**Table 6**  
LCI of cleaning CFRP.

Resources	Data	INPUT (I)/ OUTPUT (O)	I.A	I.B	I.C
Drilled CFRP part [kg]	EM	I	7.21E-03	7.21E-03	7.21E-03
Compressed air [m <sup>3</sup> ]	TD	I	1.33E-02	1.33E-02	1.33E-02
Cleaned CFRP part [kg]	EM	O	7.21E-03	7.21E-03	7.21E-03

**Table 7**  
LCI of Assembly 1.

Resources	Data	INPUT (I)/ OUTPUT (O)	I.A	I.B	I.C
Cleaned CFRP/AA7075-T6 part [kg]	EM	I/O	1.95E-02	1.95E-02	1.95E-02
Aluminum rivet [pcs]	SD	I/O	1	1	1

- FD, which represents the Fossil Depletion, and it is equivalent of the ADP<sub>f</sub>, even if the measurement unit is different.
- Land Use, which refers to the environmental effects caused by land use, and land use change, related to the FU analysed HT<sub>nc</sub>, which is the Human toxicity (non cancer) and it is partially equivalent to the HTP for the CML method.

According to the results obtained, a clear correspondence exists between CML and ReCiPe methods. This can be explained by the fact that for all the scenarios, electricity consumption mix was fixed (EU-27). Also, the most affected environmental impact categories of this study are those for which the choice of the LCIA method did not have significant implications in the comparison among the LCIA methods [35]. Also,

**Table 8**  
LCI of Pre-Assembly.

Resources	Data	INPUT (I)/ OUTPUT (O)	I.A	I.B	I.C
Total energy consumption for drilling pilot holes CFRP/AA7075-T6 [kJ]	EM	I	1.35E+ 01	1.35E+ 01	1.35E+ 01
AA7075-T6 part [kg]	EM	I	1.24E-02	1.24E-02	1.24E-02
CFRP part [kg]	EM	I	7.32E-03	7.32E-03	7.32E-03
Temporary fasteners [pcs]	SD	I	2	2	2
Energy for compressed air [kJ]	EM	I	1.23E+ 01	1.23E+ 01	1.23E+ 01
Compressed air [m <sup>3</sup> ]	TD	I	5.30E-01	5.30E-01	5.30E-01
AA7075-T6 part [kg]	EM	O	1.22E-02	1.22E-02	1.22E-02
CFRP part [kg]	EM	O	7.22E-03	7.22E-03	7.22E-03
Temporary fasteners [pcs]	SD	O	2	2	2
AA7075-T6 scrap [kg]	EM	O	8.80E-05	8.80E-05	8.80E-05
CFRP scrap [kg]	EM	O	5.20E-05	5.20E-05	5.20E-05

**Table 9**  
LCI of drilling CFRP/AA7075-T6 stack.

Resources	Data	INPUT (I)/ OUTPUT (O)	I.A	I.B	I.C
Total energy consumption for drilling CFRP/AA7075-T6 [kJ]	EM	I	5.43E+ 01	6.37E+ 01	1.51E+ 02
CFRP part [kg]	EM	I	7.22E-03	7.22E-03	7.22E-03
AA7075-T6 part [kg]	EM	I	1.22E-02	1.22E-02	1.22E-02
Energy for compressed air [kJ]	EM	I	7.45E+ 00	8.63E+ 00	2.07E+ 01
Temporary fasteners [pcs]	SD	I	2	2	2
Compressed air [m <sup>3</sup> ]	TD	I	3.24E-01	3.75E-01	9.00E-01
AA7075-T6 scrap [kg]	EM	O	1.90E-04	1.90E-04	1.90E-04
CFRP scrap [kg]	EM	O	1.12E-04	1.12E-04	1.12E-04
AA7075-T6 part [kg]	EM	O	1.20E-02	1.20E-02	1.20E-02
CFRP part [kg]	EM	O	7.11E-03	7.11E-03	7.11E-03
Temporary fasteners [pcs]	SD	O	2	2	2

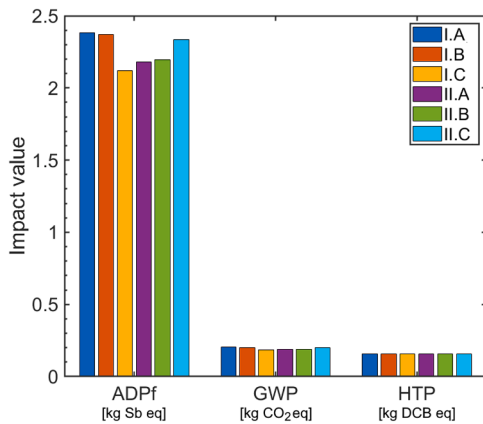
similar trends among the different scenarios were observed in terms of environmental impact categories. In particular, the best case is always the I.C scenario whereas the worst case is the I.A scenario, in terms of environmental impact.

Table 12 summarizes the best- and worst-performing scenarios for the most representative environmental impact categories identified through the CML and ReCiPe 2016 methods.

The pie chart in Table 8 shows the GWP for the best scenario, which is representative of all the scenarios since all the other subscenarios

**Table 10**  
LCI of cleaning CFRP/AA7075-T6 stack.

Resources	Data	INPUT (I)/ OUTPUT (O)	II.A	II.B	II.C
Drilled CFRP/ AA7075-T6 part [kg]	EM	I	1.91E-02	1.91E-02	1.91E-02
Temporary fasteners [pcs]	EM	I	2	2	2
Cleaned CFRP/ AA7075-T6 part [kg]	EM	O	1.91E-02	1.91E-02	1.91E-02
Temporary fasteners [pcs]	SD	O	2	2	2
Compressed air [m <sup>3</sup> ]	EM	I	1.33E-02	1.33E-02	1.33E-02
Energy for compressed air [kJ]	EM	I	3.06E-01	3.06E-01	3.06E-01



**Fig. 6.** CML 2016 results of all the gate-to-gate scenarios.

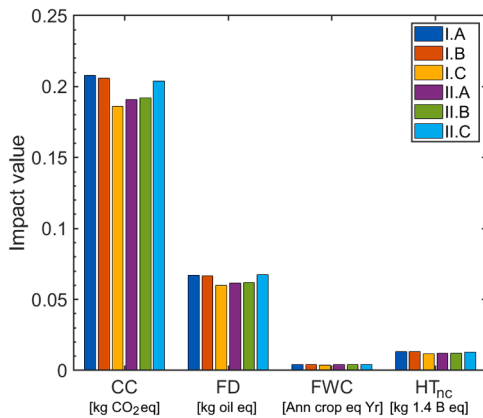


**Fig. 7.** ReCiPe 2016 – Midpoint (H) results of all the gate-to-gate scenarios.

**Table 11**  
LCI of Assembly 2.

Resources	Data	INPUT (I)/ OUTPUT (O)	II.A	II.B	II.C
Cleaned CFRP/ AA7075-T6 part [kg]	EM	I/O	1.91E-02	1.91E-02	1.91E-02
Aluminum rivet [pcs]	SD	I/O	1	1	1

showed percentage results that are intermediary between the two

**Table 12**  
Summary of best and worst drilling scenarios for key environmental impact categories (CML and ReCiPe 2016 methods).

Impact Category	Best Case (Scenario)	Worst Case (Scenario)
<b>CML</b>		
ADPF [kg Sb eq.]	2.12E+ 00 (I.C)	2.38E+ 00 (I.A)
GWP [kg CO <sub>2</sub> eq.]	1.83E-01 (I.C)	2.03E-01 (I.A)
HTP [kg DCB eq.]	1.56E-01 (I.C/II.A/II.B/II.C)	1.57E-01 (I.A/I.B)
<b>ReCiPe</b>		
CC [kg CO <sub>2</sub> eq.]	1.86E-01 (I.C)	2.08E-01 (I.A)
FD [kg oil eq.]	6.00E-02 (I.C)	6.90E-02 (II.C)
HT <sub>nc</sub> [kg 1,4 B eq.]	3.91E-03 (I.C)	4.35E-03 (I.A)
LU [Ann crop eq. Yr]	1.15E-02 (I.C)	1.34E-02 (I.A)

displayed pie charts. In all the investigated subscenarios, CFRP production required the greatest amount of energy consumption. The global contribution of drilling, cleaning and assembly to the GWP goes from 4 % to 14 % selecting the worst-case process conditions rather than the best ones.

These results can be explained considering that in all the scenarios investigated in this work, only the drilling process varies in terms of resources used for the LCA. That means that all the differences which can be observed in terms of LCIA are allocated to that process.

In this regard, power and energy consumption of drilling operations were estimated as described in the 2.3 subsection. Total energy consumption  $E_{TOT}$  for drilling was given as the sum of two contributions:  $E_{CNC}$  and  $E_{motor}$ .

- $E_{CNC}$ , which is given as the product of the nominal power of the machine (23 kW) and the time needed for drilling according to the selected process conditions. Thus, this contribution is dependent exclusively on the drilling time. The longer the drilling duration, the higher the  $E_{CNC}$ . It is important to underline that considering a constant value of the power over drilling time,  $E_{CNC}$  can be overestimated.
- $E_{motor}$  is dependent on the process parameters and so on the cutting forces involved, because of the interaction of the tool with the material, as well as on the drilling time.

**Fig. 9** depicts the  $E_{TOT}$  for all the scenarios investigated. It can be observed that scenario I.A and I.B are the most energy-intensive, followed by subscenario II.C. For those three subscenarios,  $E_{TOT}$  ranges between 150 and 200 kJ. Conversely, subscenario II.A and II.B required an amount of total energy consumption of around 50 kJ. The best result was achieved by subscenario I.C. Thus, according to the results obtained in this work, the combination of the process parameters resulting in maximum active power during the drilling of AA7075-T6 and CFRP (in single-material drilling strategy) before their assembly led to around 80 % reduction of the energy consumption for a single hole.

According to **Eq. 2**,  $E_{CNC}$  variations only depend on the drilling time. Instead  $E_{motor}$  depends on two distinct factors which are the drilling time and power consumption. **Fig. 10a** shows the spindle motor energy for each drilling time, deriving from the selected process conditions. A linear relationship correlates  $E_{motor}$  with the drilling time; thus, for the selected materials, drilled under the above-mentioned process parameters, drilling time affects the energy consumption more than the power consumption and so the forces involved. **Fig. 10b** depicts the  $E_{motor}$  for all the investigated scenarios. It can be observed that scenario I.C led to the highest spindle motor energy. For the subscenarios I.A, I.B and I.C, the results are inverse to those can be observed in **Fig. 9**. That means that the  $E_{air}$  plays a crucial role in the  $E_{TOT}$ . Conversely, for the subscenarios II.A, II.B and II.C,  $E_{TOT}$  follows the trend of the  $E_{motor}$ . That means that  $E_{air}$

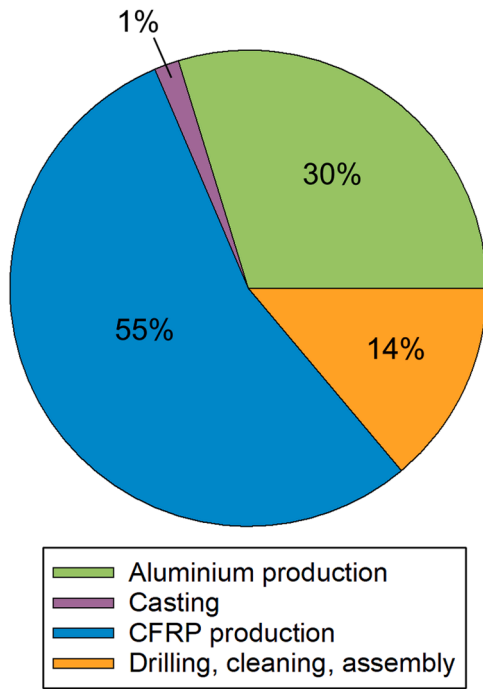


Fig. 8. Percentage of the stage's contribution to the GWP of scenario I.A.

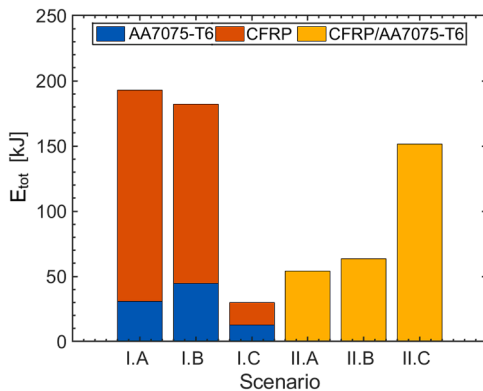


Fig. 9. Energy consumption for a single-hole drilling for all the investigated scenarios.

follows the same trend as well by varying the scenario.

As mentioned above, the LCA analysis carried out in this work focuses on the comparative assessment of drilling processes across two distinct operating scenarios to understand the differences in environmental impact between drilling configurations typically used in the aerospace industry. Since machine manufacturing and transportation are similar in the two scenarios examined and do not vary significantly, their overall impact was considered negligible for this study, thus not altering the conclusions. Furthermore, excluding these phases allows the analysis to focus on the direct machining phases, which are the elements of greatest interest for comparing different drilling strategies. Future extensions of the analysis will include a more comprehensive assessment that also takes into account the manufacturing and transportation phases.

### 3.2. Joint analysis of drilling quality and environmental impact

The assessment of drilling strategies for CFRP/aluminium stacks assembly must concurrently address two critical aspects: the quality of the drilled holes and the environmental footprint associated with the

drilling operation. In the present study, this dual perspective was achieved by analysing the hole quality indicators and directly correlating them with the energy demand of each drilling condition included in the LCA. The results of the LCA analyses showed that scenario I.C (i.e.  $v_c = 140$  m/min and  $f = 0.125$  mm/rev for AA7075-T6 and  $v_c = 120$  m/min and  $f = 0.070$  mm/rev for CFRP) was the most favourable in terms of energy consumption and global environmental impact. Table 13 reports quality results for the combinations investigated in this work. Quality data reveal that the process conditions adopted for subscenario I.C, corresponding to combination 3 for AA7075-T6 and combination 6 for CFRP, produced the worst outcome in terms of overall hole quality.

Hole quality indicators were extracted from the experimental results reported in [25], for all nine drilling conditions considered in this work. Specifically, for AA7075-T6 and CFRP, quality was assessed through burr height (top and bottom) and delamination factor, respectively, while surface roughness was considered for both materials. For the CFRP laminate, the delamination factor was calculated at the hole exit side using optical analysis with a Keyence VHX-7000 digital microscope. The maximum delaminated diameter ( $D_{max}$ ) was measured and compared to the nominal hole diameter ( $D_n$ ), applying the commonly adopted expression:

$$F_d = \frac{D_{max}}{D_n} \tag{5}$$

The maximum burr height was measured at both hole entry and exit on AA7075-T6 and was acquired via Sensofar S Neox confocal microscope. Similarly, surface roughness ( $R_a$ ) was measured on the internal hole wall using a MarSurf PS10 by Mahr contact profilometer according to ISO 3274. For stacks, the evaluation of hole quality focused on the specific indicators that were found to be affected by the drilling parameters in [25] (burr height at both entry and exit, delamination factor, and surface roughness).

In the subscenario I.A, corresponding to the best quality conditions for both AA7075-T6 and CFRP, the holes exhibited minimal burr formation and low delamination, with low surface roughness values. These favourable quality outcomes, however, entailed the highest total energy consumption among the single-material drilling strategy ( $E_{TOT} = 193.0$  kJ). This finding highlights a common industrial trade-off: pursuing optimal hole quality can entail significant energy and productivity penalties. In practice, such a solution may be viable only when hole integrity is a critical requirement, such as in safety-critical aerospace joints or when no post-processing (e.g., deburring) is possible. Conversely, scenario I.B, based on minimum active power consumption, showed a significant deterioration in quality, particularly in terms of bottom burr height, while the delamination factor remained close to that observed in I.A. The total energy consumption was slightly lower ( $E_{TOT} = 182.0$  kJ), this highlights that a lower instantaneous power demand does not necessarily translate into improved overall energy performance or optimal quality, particularly in the metallic layer. In scenario I.C, which corresponds to the highest tested combination of cutting speed and feed rate, a clear degradation of hole quality was observed. Compared to subscenario I.A, the surface roughness of CFRP increased by approximately sixfold, while the height of the bottom burr in AA7075-T6 increased ninefold. The delamination factor also showed a slight increase of 9.4%. As discussed in [25], high feed rates and cutting speeds tend to amplify thermo-mechanical loads at the tool-workpiece interface, promoting fibre-matrix damage in CFRP and increasing the plastic deformation at the tool exit in aluminium, thus favouring burr formation. In this context, the overall surface integrity was significantly compromised. Interestingly, despite these quality losses, scenario I.C recorded the lowest total energy consumption among all cases where the single-material drilling strategy has been adopted ( $E_{TOT} = 30.0$  kJ), primarily due to the reduced drilling time. This makes I.C potentially attractive when high productivity and low energy usage are prioritized over quality, such as for pilot holes or non-structural components.

The one-shot strategy (II.A, II.B, II.C) displayed different quality

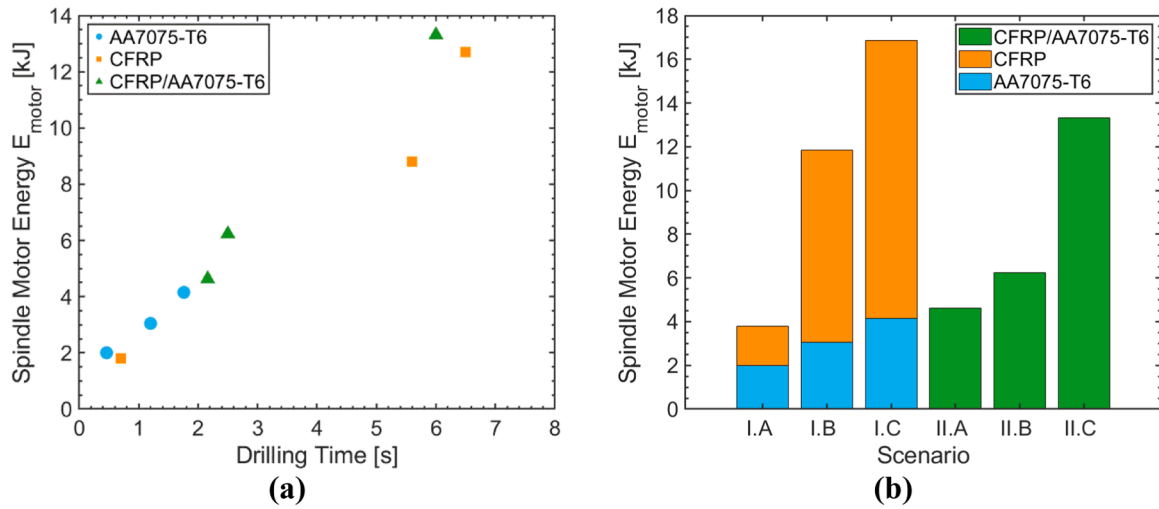


Fig. 10. (a) Scatter plot of drilling time vs. spindle motor energy for AA7075-T6, CFRP, and CFRP/AA7075-T6 stack; (b) Stacked bar chart showing  $E_{\text{motor}}$  contributions per scenario.

Table 13  
Quality results for the combinations investigated in this work.

Selection Criterion	Material	Burr height <sub>t</sub> [mm]	Burr height <sub>b</sub> [mm]	Delamination Factor	Roughness [μm]
BHQ	AA7075-T6	0.021	0.019	–	0.486
MnAP	AA7075-T6	0.018	0.491	–	0.480
MxAP	AA7075-T6	0.033	0.178	–	0.606
BHQ	CFRP	–	–	1.057	0.410
MnAP	CFRP	–	–	1.167	0.382
MxAP	CFRP	–	–	1.067	2.602
CP-AA	CFRP/AA7075-T6	0.027	0.013	1.034	2.623 (CFRP) 0.390 (AA7075-T6)
CP-CFRP	CFRP/AA7075-T6	0.019	0.123	1.030	2.641 (CFRP) 0.413 (AA7075-T6)
APS	CFRP/AA7075-T6	0.009	0.016	1.028	0.599 (CFRP) 0.459 (AA7075-T6)

outcomes while maintaining energy consumption values comparable with those achieved in the case of the single-material drilling scenarios. Scenario II.A, based on compromise parameters favouring aluminium, resulted in the lowest burr height at the aluminium exit among all subscenarios and a moderate delamination factor. Despite this, the total energy consumption of subscenario II.A remained limited to 54.31 kJ, which represents a reduction of 71.9 % and 70.2 % compared to the single-material drilling sequences I.A and I.B, respectively. However, it was still 80.5 % higher than the minimum energy scenario I.C (30.08 kJ). This suggests that parameter compromise in favour of the more ductile material can lead to satisfactory performance without excessive energy costs, and might be suitable for general-purpose drilling in hybrid stacks. Subscenario II.B, representing the compromise strategy oriented toward CFRP, exhibited an improved roughness for the composite layer, albeit only marginally better than II.A, and a slightly lower delamination factor. However, the bottom burr height on AA7075-T6 increased substantially to 0.12285 mm, exceeding the

threshold of 0.10 mm for structural applications. Scenario II.C, based on the dynamic parameter switching strategy, demonstrated a more favourable trade-off. It achieved the absolute minimum in both bottom burr height (0.016 mm) and delamination factor ( $F_d = 1.028$ ), while surface roughness in CFRP was drastically reduced ( $R_a = 0.599 \mu\text{m}$ ), representing a decrease of 77 % compared to II.A. These results highlight the effectiveness of the adaptive approach in mitigating interface-related damage, particularly at the critical transition between dissimilar materials. In the context of one-way assembly processes, where drilled components are not disassembled for deburring or interface rework, subscenario II.C offers a strategically superior solution. However, this improvement in quality was accompanied by a substantial energy penalty: the total energy consumption ( $E_{\text{TOT}} = 151.31 \text{ kJ}$ ) was more than five times higher than in the subscenario I.C, which recorded the lowest energy demand among all tested conditions ( $E_{\text{TOT}} = 30.08 \text{ kJ}$ ).

A more comprehensive comparison across all six drilling scenarios is presented in the radar chart shown in Fig. 11, where each quality indicator was normalised with respect to its maximum value. Subscenario I.A confirms its superiority in terms of quality, presenting the most balanced profile across nearly indicators. Conversely, subscenario I.C, while showing excellent performance in terms of total drilling energy  $E_{\text{TOT}}$  and Specific Cutting Energy (SCE), exhibits the worst values for surface roughness  $R_a$  in CFRP and a significant increase in burr height at the aluminium exit. Fig. 11 thus reinforces the conclusion that energy

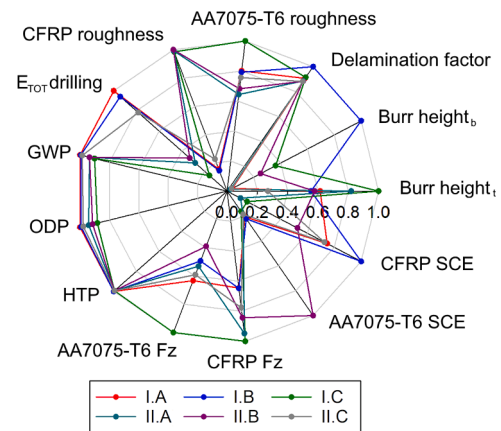


Fig. 11. Effect of the different process conditions for both drilling strategy on hole quality and LCIA results.

saving and productivity gains achieved through high feed rate and cutting speed come at the expense of quality integrity. A key consideration emerging from this analysis is the high thrust force measured in scenario I.C, 234.8 N for AA7075-T6 and 49.0 N for CFRP, representing the highest values among all subscenarios. This is a particularly relevant point, as thrust force is strongly correlated with tool wear progression, which has direct consequences on process sustainability. Several studies have demonstrated that elevated thrust forces exacerbate abrasive wear in CFRP and plastic deformation in aluminium, accelerating both flank wear and cutting-edge chipping. For instance, Montoya et al. [39] observed that increased thrust force significantly impacted wear rate on uncoated tungsten carbide tools when drilling CFRP/Aluminium stacks, leading to rapid tool degradation and compromised hole quality. Similarly, Bai et al. [40] quantitatively confirmed that higher thrust forces correlate directly with increased tool wear in unidirectional CFRP laminates, causing a rise in defects such as delamination and fiber pull-out. Dahnel et al. [41] observed that in aluminium drilling, thrust force is primary driver of tool wear evolution, especially in dry conditions, and directly contributes to excessive burr formation and surface damage. Similarly, Alagan et al. [30] highlighted that high thrust forces in CFRP/Aluminium hybrid drilling exacerbate tool abrasion and thermal damage, which accelerates the loss of tool sharpness and negatively affects hole integrity. Therefore, although scenario I.C appears energetically optimal, the high thrust force values suggest an increased risk of premature tool degradation. In practical applications, this could result in higher tool replacement costs. Among the one-shot scenarios, II.A offers moderate thrust force and the lowest burr height at the aluminium exit. Despite a slightly higher  $E_{TOT}$  than subscenario I.C, II.A offers a more favourable quality profile, particularly in terms of deburring requirements. Subscenario II.B, with parameters favouring CFRP, achieves good delamination control and lower thrust force in the composite layer (41.29 N), but suffers from elevated burr height in aluminium, exceeding the typical aerospace threshold of 0.10 mm. Such a condition could impair assembly precision, requiring secondary deburring operations and increasing production time and cost. Subscenario II.C, based on the adaptive switching of drilling parameters at the material interface, emerges as the most effective in terms of hole quality across both materials. It achieves the lowest recorded values of burr height and delamination factor, while also maintaining thrust forces at moderate levels (138.86 N for AA7075-T6 and 38.01 N for CFRP).

Ultimately, the radar chart analysis underscores the need to balance energy and quality indicators when selecting drilling strategies. While subscenarios like I.C may seem advantageous from a purely environmental standpoint, their implications in terms of thrust force and accelerated tool wear, as clearly demonstrated in the literature, cannot be overlooked.

**4. Conclusions**

This study provided a comprehensive environmental and technical assessment of different drilling strategies for CFRP/AA7075-T6 hybrid stacks, integrating experimental data into a cradle-to-gate Life Cycle Assessment (LCA) framework. The goal was to evaluate both sustainability and machining performance in different drilling strategies and to offer actionable insights for industries that are interested to these stacks. The key outcomes can serve as decision-making guidelines depending on the primary objective, whether energy efficiency, hole quality, or process balance is prioritized.

The following conclusions can be drawn:

- LCA results showed that the drilling process contributes between 4 % and 14 % of the total GWP, depending on the drilling strategy and process parameters. The most sustainable outcomes, reflected in indicators such as ADP<sub>f</sub>, AP, GWP, CC, FD, and FWEP, were obtained with the single-material drilling strategy using parameters that maximize active power and minimize the machining time, thus

minimizing the energy demand of the CNC auxiliary systems  $E_{CNC}$ . The second-best performance was observed with the one-shot strategy using aluminium-favoured parameters (subscenario II.A,  $v_c=60$  m/min and  $f=0.075$  mm/rev).

- The use of the single-material drilling strategy with the parameters minimizing total energy consumption and SCE showed the worst quality: a sixfold increase in surface roughness in CFRP and a ninefold increase in burr height in aluminium, compared to the best-quality subscenario was observed.
- The use of the one-shot drilling with the adaptive parameter switching strategy resulted in the highest energy demand, with a fivefold increase over I.C subscenario, but offered the best overall hole quality, achieving a delamination factor of 1.028 and top burr height of 0.009 mm.
- Among all holes obtained using the single-material drilling strategy, those produced with parameters that maximize hole quality for each material resulted in the lowest burr height and delamination, but required the highest energy consumption, even higher than that of the one-shot strategies. This subscenario, along with I.B (using parameters to minimize the active power, i.e.  $v_c=60$  m/min and  $f=0.050$  mm/rev for AA7075-T6 and  $v_c=50$  m/min and  $f=0.010$  mm/rev for CFRP), also yielded the worst environmental indicators.
- High thrust forces (e.g., in I.C) suggest accelerated tool wear and related environmental impacts due to increased tool consumption. Conversely, lower forces were recorded in the minimum-power strategy (I.B subscenario), point to better sustainability in extended use. The adaptive switching approach achieved moderate thrust forces, offering a compromise between wear and quality.

From a strategic perspective, drilling strategy selection should be tailored to the objective function:

- For minimum environmental impact, it is recommended to use the single-material drilling strategy using the parameters that maximize the maximum active power but consider quality compromises and tool wear.
- For best overall hole quality, it is recommended to use of the one-shot drilling strategy with adaptive parameter switching, accepting higher energy consumption but moderate drilling forces.
- For balanced performance (energy, quality and environmental indicators), it is recommended to use the one-shot drilling strategy without switching, applying aluminium-optimised parameters, a practical solution with reduced deburring and stable thrust forces.

In summary, this study demonstrates that no single drilling condition is universally optimal. A multi-criteria selection approach, considering quality, energy consumption, and mechanical integrity, is essential. The insights provided herein may serve as process guidelines for selecting drilling strategies based on specific manufacturing goals.

**List of abbreviations**

Abbreviation	Definition	Unit
LCA	Life Cycle Assessment	
LCIA	Life Cycle Impact Assessment	
LCI	Life Cycle Inventory	
FU	Functional Unit	
CNC	Computer Numerical Control	
NCU	Numerical Control Unit	
CP-AA	Compromise Parameters – Aluminium favoured	
CP-CFRP	Compromise Parameters – CFRP favoured	
APS	Adaptive Parameter Switching	
BHQ	Best Hole Quality	
MnAP	Minimum Active Power	
MxAP	Maximum Active Power	
SCE	Specific Cutting Energy	

(continued on next page)

(continued)

$E_{TOT}$	Total Energy Consumption	kJ
MRR	Material Removal Rate	mm <sup>3</sup> /min
$R_a$	Surface Roughness	µm
$F_d$	Delamination Factor	
$v_c$	Cutting Speed	m/min
$f$	Feed Rate	mm/rev
$v_a$	Feed Speed	mm/min
$n$	Rotational Speed	rpm
CFRP	Carbon Fibre Reinforced Polymer	
AA7075-T6	Aluminium Alloy 7075-T6	
CVD	Chemical Vapor Deposition	
$F_z$	Thrust Force	N
$M_z$	Torque	Nm

### CRedit authorship contribution statement

**Luca Boccarusso:** Writing – review & editing, Supervision, Project administration, Conceptualization. **Martina Panico:** Writing – review & editing, Writing – original draft, Visualization, Validation, Methodology, Investigation, Formal analysis, Data curation, Conceptualization. **Antonello Astarita:** Writing – review & editing, Supervision, Project administration, Conceptualization. **Ersilia Cozzolino:** Writing – review & editing, Writing – original draft, Validation, Software, Methodology, Investigation, Formal analysis, Conceptualization. **Andreas Gebhardt:** Resources, Funding acquisition. **Bagemann Eva:** Resources, Funding acquisition.

### Declaration of Competing Interest

The authors declare that they have no known competing financial interests or personal relationships that could have appeared to influence the work reported in this paper.

### Appendix A. Supporting information

Supplementary data associated with this article can be found in the online version at [doi:10.1016/j.cirpj.2025.12.001](https://doi.org/10.1016/j.cirpj.2025.12.001).

### References

- Khanna N, Wadhwa J, Pitroda A, et al. Life cycle assessment of environmentally friendly initiatives for sustainable machining: A short review of current knowledge and a case study. *Sustain Mater Technol* 2022;32:e00413. <https://doi.org/10.1016/j.susmat.2022.e00413>.
- Lei H, Zhao L, Cheng J, et al. Material removal mechanisms affected by milling modes for defective KDP surfaces. *CIRP J Manuf Sci Technol* 2024;48:67–83. <https://doi.org/10.1016/j.cirpj.2023.11.008>.
- Uçak N, Outeiro J, Çiçek A, Aslantas K. Comparative analysis of micro-milling performances of conventionally and additively manufactured Ti6Al4V alloys: Experimental investigation and 3D modelling. *CIRP J Manuf Sci Technol* 2024;51: 213–35. <https://doi.org/10.1016/j.cirpj.2024.05.003>.
- Qiu Z, Tang J, Li Z, et al. The influence of magnetic field controlled electrical discharge milling on the surface quality of grooves. *CIRP J Manuf Sci Technol* 2025;59:98–117. <https://doi.org/10.1016/j.cirpj.2025.03.006>.
- Mayer P, Kirsch B, Müller C, et al. Deformation induced hardening when cryogenic turning. *CIRP J Manuf Sci Technol* 2018;23:6–19. <https://doi.org/10.1016/j.cirpj.2018.10.003>.
- Denkena B, Krödel A, Heckemeyer A. Numerical and experimental analysis of thermal and mechanical tool load when turning AISI 52100 with ground cutting edge microgeometries. *CIRP J Manuf Sci Technol* 2021;35:494–501. <https://doi.org/10.1016/j.cirpj.2021.08.006>.
- Nakagawa J, Farahani ND, Altintas Y. Identification and effect of chip shear band on chatter vibration in the turning of Nickel Alloy 718. *CIRP J Manuf Sci Technol* 2023;44:82–90. <https://doi.org/10.1016/j.cirpj.2023.05.004>.
- Martínez Herrero E, Pereda Pereda L, Huidobro Fernández F, et al. An environmental evaluation of a milling machine range: a case study on reconfigurable approach. *SN Appl Sci* 2019;1:1513. <https://doi.org/10.1007/s42452-019-1552-7>.
- Fernando WLR, Karunathilake HP, Gamage JR. Strategies to reduce energy and metalworking fluid consumption for the sustainability of turning operation: A review. *Clean Eng Technol* 2021;3:100100. <https://doi.org/10.1016/j.clet.2021.100100>.
- Mei B, Zhu W. Accurate positioning of a drilling and riveting cell for aircraft assembly. *Robot Comput Integr Manuf* 2021;69:102112. <https://doi.org/10.1016/j.rcim.2020.102112>.
- Jebaratnam JM, Hassan MH. Comprehensive review of drilling strategies for CFRP/Ti stacks in aircraft manufacturing. *Mach Sci Technol* 2025;1–105. <https://doi.org/10.1080/10910344.2025.2475484>.
- Gangi F, Mustilli M, Daniele LM, Coscia M. The sustainable development of the aerospace industry: Drivers and impact of corporate environmental responsibility. *Bus Strategy Environ* 2022;31:218–35. <https://doi.org/10.1002/bse.2883>.
- Rodrigues Dias VM, Jugend D, de Camargo Fiorini P, et al. Possibilities for applying the circular economy in the aerospace industry: Practices, opportunities and challenges. *J Air Transp Manag* 2022;102:102227. <https://doi.org/10.1016/j.jairtraman.2022.102227>.
- Kayihan M, Karaguzel U, Bakkal M. Process design and experimental study on drilling operations of a hybrid aluminum/carbon fiber reinforced polymer/titanium composite. *Mater Manuf Process* 2024;39:1630–7. <https://doi.org/10.1080/10426914.2024.2368547>.
- Xu J, Ji M, Chen M, El Mansori M. Experimental investigation on drilling machinability and hole quality of CFRP/Ti6Al4V stacks under different cooling conditions. *Int J Adv Manuf Technol* 2020;109:1527–39. <https://doi.org/10.1007/s00170-020-05742-8>.
- Panico M, Durante M, Langella A, Boccarusso L. One-shot drilling process for thin CFRP/Aluminium alloys stacks. *Mater Manuf Process* 2024;1–16. <https://doi.org/10.1080/10426914.2024.2311383>.
- Xu J, Geier N, Shen J, et al. A review on CFRP drilling: fundamental mechanisms, damage issues, and approaches toward high-quality drilling. *J Mater Res Technol* 2023;24:9677–707. <https://doi.org/10.1016/j.jmrt.2023.05.023>.
- Campitelli A, Cristóbal J, Fischer J, et al. Resource efficiency analysis of lubricating strategies for machining processes using life cycle assessment methodology. *J Clean Prod* 2019;222:464–75. <https://doi.org/10.1016/j.jclepro.2019.03.073>.
- Khanna N, Shah P, Wadhwa J, et al. Energy Consumption and Lifecycle Assessment Comparison of Cutting Fluids for Drilling Titanium Alloy. *Procedia CIRP* 2021;98: 175–80. <https://doi.org/10.1016/j.procir.2021.01.026>.
- Shah P, Bhat P, Khanna N. Life cycle assessment of drilling Inconel 718 using cryogenic cutting fluids while considering sustainability parameters. *Sustain Energy Technol Assess* 2021;43:100950. <https://doi.org/10.1016/j.seta.2020.100950>.
- Khanna N, Prajapati R, Bolar G. Fabrication, machining (dry vs. cryogenic) and life cycle analysis of hybrid titanium composite laminates (HTCL). *Mach Sci Technol* 2024;28:626–55. <https://doi.org/10.1080/10910344.2024.2369856>.
- Zhu M, Ouyang J, Tian Y, et al. Understanding factors affecting the process efficiency, quality and carbon emission in laser drilling of CFRP composite via tailored sequence multiple-ring scanning. *Compos B Eng* 2024;272:111156. <https://doi.org/10.1016/j.compositesb.2023.111156>.
- Zhu M, Guo W, Ouyang J, et al. Low carbon high quality simultaneous laser and mechanical hybrid drilling of carbon fibre reinforced polymer composite. *CIRP J Manuf Sci Technol* 2023;46:1–18. <https://doi.org/10.1016/j.cirpj.2023.07.003>.
- Kang YS, Kim DE, Park HW, Seo J. Sustainable CFRP drilling using support plates: A comprehensive analysis of delamination suppression and cost-effectiveness. *Mater Today Sustain* 2025;30:101085. <https://doi.org/10.1016/j.mtsust.2025.101085>.
- Panico M, Begemann E, Gebhardt A, et al. Process parameter auto-adaptation strategy for one-up drilling of CFRP/aluminium hybrid stack. *Int J Adv Manuf Technol* 2024. <https://doi.org/10.1007/s00170-024-14753-8>.
- Betgül Ç, Köklü U, Morkavuk S. The effects of support plate thickness on the drilling machinability of CFRP. *J Reinf Plast Compos* 2023. <https://doi.org/10.1177/07316844231218942>.
- Cozzolino E, Franchitti S, Borrelli R, et al. Energy consumption assessment in manufacturing Ti6Al4V electron beam melted parts post-processed by machining. *Int J Adv Manuf Technol* 2023;125:1289–303. <https://doi.org/10.1007/s00170-022-10794-z>.
- Zitoun R, Krishnaraj V, Collombet F. Study of drilling of composite material and aluminium stack. *Compos Struct* 2010;92:1246–55. <https://doi.org/10.1016/j.compstruct.2009.10.010>.
- Zhang L, Liu Z, Tian W, Liao W. Experimental studies on the performance of different structure tools in drilling CFRP/Al alloy stacks. *Int J Adv Manuf Technol* 2015;81:241–51. <https://doi.org/10.1007/s00170-015-6955-z>.
- Tamil Alagan N, Sajja NT, Gustafsson A, et al. Investigation of the quality of Al-CFRP stacks when drilled using innovative approaches. *CIRP J Manuf Sci Technol* 2023;43:260–72. <https://doi.org/10.1016/j.cirpj.2023.04.011>.
- Bertolini R, Alagan NT, Gustafsson A, et al. Ultrasonic Vibration and Cryogenic assisted drilling of Aluminum-CFRP Composite Stack – An innovative approach. *Procedia CIRP* 2022;108:94–9. <https://doi.org/10.1016/j.procir.2022.03.020>.
- Wang C, Cheng K, Rakowski R, et al. Comparative studies on the effect of pilot drillings with application to high-speed drilling of carbon fibre reinforced plastic (CFRP) composites. *Int J Adv Manuf Technol* 2017;89:3243–55. <https://doi.org/10.1007/s00170-016-9268-y>.
- ISO 14040. 2006 - Environmental management — Life cycle assessment — Principles and framework. International Organization for Standardization; 2006. p. 1–20.
- ISO 14044. 2006 - Environmental management — Life cycle assessment — Requirements and guidelines. International Organization for Standardization; 2006. p. 1–46.
- Rybczewska-Błażejowska M, Jezierski D. Comparison of ReCiPe 2016, ILCD 2011, CML-IA baseline and IMPACT 2002+ LCIA methods: a case study based on the

- electricity consumption mix in Europe. *Int J Life Cycle Assess* 2024;29:1799–817. <https://doi.org/10.1007/s11367-024-02326-6>.
- [36] Humbert S, Rossi V, Margni M, et al. Life cycle assessment of two baby food packaging alternatives: glass jars vs. plastic pots. *Int J Life Cycle Assess* 2009;14: 95–106. <https://doi.org/10.1007/s11367-008-0052-6>.
- [37] João Vasco de Oliveira Fernandes Lopes. *Life Cycle Assessment of the Airbus A330-200 Aircraft*. Instituto Superior Técnico - Universidade de Lisboa; 2010.
- [38] Cozzolino E, Astarita A, De Luca M, Sinagra C. Life cycle assessment of the rolling process of thin aluminum sheets. *Mater Manuf Process* 2024;39:2237–52. <https://doi.org/10.1080/10426914.2024.2395004>.
- [39] Montoya M, Calamaz M, Gehin D, Girot F. Evaluation of the performance of coated and uncoated carbide tools in drilling thick CFRP/aluminium alloy stacks. *Int J Adv Manuf Technol* 2013;68:2111–20. <https://doi.org/10.1007/s00170-013-4817-0>.
- [40] Bai Y, Jia Z yuan, Fu R, et al. Mechanical model for predicting thrust force with tool wear effects in drilling of unidirectional CFRP. *Compos Struct* 2021;262. <https://doi.org/10.1016/j.compstruct.2021.113601>.
- [41] Dahnel AN, Fauzi MH, Raof NA, et al. Tool wear and burr formation during drilling of aluminum alloy 7075 in dry and with cutting fluid. *Mater Today Proc* 2022;59: 808–13. <https://doi.org/10.1016/j.matpr.2022.01.110>.